Mathematical Models and Methods in Applied Sciences

COMPARTMENTAL MODELLING OF SOCIAL DYNAMICS WITH GENERALISED PEER INCIDENCE

J. J. BISSELL, C. C. S. CAIADO, M. GOLDSTEIN, AND B. STRAUGHAN

Department of Mathematical Sciences, University of Durham, Durham City, County Durham, DH1 3LE, United Kingdom

Received (Day Month Year)
Revised (Day Month Year)
Communicated by (xxxxxxxxxx)

A generalised compartmental method for investigating the spread of socially determined behaviour is introduced, and cast in the specific context of societal smoking dynamics with multiple peer influence. We consider how new peer influence terms, acting in both the rate at which smokers abandon their habit, and the rate at which former smokers relapse, can affect the spread of smoking in populations of constant size. In particular, we develop a three-population model (comprising classes of potential, current, and former smokers) governed by multiple incidence transfer rates with linear frequency dependence. Both a deterministic system and its stochastic analogue are discussed: in the first we demonstrate that multiple peer influence not only modifies the number of steady-states and nature of their asymptotic stability, but also introduces a new kind of non-linear 'tipping-point' dynamic; while in the second we use recently compiled smoking statistics from the Northeast of England to investigate the impact of systemic uncertainty on the potential for societal 'tipping'. The generality of our assumptions mean that the results presented here are likely to be relevant to other compartmental models, especially those concerned with the transmission of socially determined behaviours.

Keywords: Mathematical Modelling of Social Systems; Deterministic and Stochastic Compartmental Models; Smoking Dynamics; Bi-stability; Sensitivity Analysis

AMS Subject Classification: 92B99, 91D99, 60H10, 92C99, 34D20

1. Introduction

The modelling of epidemic outbreaks and spread of disease has been investigated for centuries. Early studies tried to explain the dispersion of bubonic plague and cholera through observational analysis of mortality data; one of the first mathematical attempts being Daniel Bernoulli's seminal 1766 work on smallpox.[5] In 1927, Kermack and McKendrick introduced a deterministic compartmental model to characterise the behaviour of population subgroups during an epidemic.[16] Due to the relative simplicity of their approach, and its success in describing historical outbreaks, it has been widely applied and modified to incorporate new groups, behaviours and stochastic aspects. Indeed, though developed to predict the spread of infectious disease, recent years have seen a general movement amongst authors

who—keen to capitalise on the success of the compartmental method—are adapting epidemiology approaches to model the transmission of 'infectious' behavioural patters in human society, especially those considered addictive or undesirable, such as cigarette smoking and binge drinking.[9,19,22,23,28,31,34] The status of smoking as a high profile public health risk[35] means that modelling societal smoking dynamics in terms of behaviour transmission is particularly topical.[19,31]

In this article we generalise a basic compartmental 'behaviour transmission' model to include incidence terms describing multiple 'peer influence' effects, that is, the tendency for individuals to follow social norms: either passively, through 'peer imitation'; or actively, in response to encouragement ('peer pressure')[11,27]. Though frequently cited as important factors in the spread of many behavioural trends, these kinds of influences tend to feature in mathematical models only as part of initial uptake (cf. infection)[10,19,22,23,31]; their impact on other aspects of behavioural transmission is rarely considered, and then limited to rates of behaviour relapse (see, for example, the heroin and bulimia models of White-Comiskey[34] and González *et al.*[9] respectively). Indeed, to our knowledge, the effect of peer influence on the rate at which individuals abandon a given practice is yet to be considered, an omission we shall give special attention. Note that we use the term 'peer influence' in a broad sense to mean the effect on a given individual of the behaviour of those with whom he or she has contact—be they relatives, friends, colleagues, teachers, students, strangers, etc.—and no particular group is assumed.

As a working example, we develop a three population compartmental model to describe the spread of cigarette smoking, a context in which we expect peer influence to play a significant role in the rate of both uptake and cessation of habit[11,27]: intuitively one imagines that smokers will be more eager to give up smoking if censured by popular opinion, just as former smokers are more likely to relapse when in regular contact with people who smoke. However, while cast in terms of smoking, our model is quite general, and likely to find application in other kinds of behavioural transmission systems (e.g., those in references [9, 22, 23, 34]).

Given the need to discuss a number of deterministic and stochastic aspects, what follows is broadly speaking divided into two parts. We begin by developing the underlying deterministic model (§2), describing its basic properties exclusive of generalised peer influence in §3, where we determine the system's steady-states and their linear stability. The new peer influence terms are added to the model in §4, a generalisation which we show leads to very different steady-state characteristics (when compared to the results in §3), and novel 'tipping-point' behaviour, whereby small changes to certain parameters can force dramatic shifts in system dynamics. To determine the systemic uncertainty in our model, and to better assess the potential for societal 'tipping', we analyse the model stochastically in §5; this section includes an investigation into the sensitivity of both the deterministic and stochastic methods. Further developments and generalisations of the model, and future possibilities for combined deterministic and stochastic approaches to modelling behavioural transmission dynamics are considered in section 6.

2. Three Population Compartmental Model

The basic approach in what we describe as 'behaviour transmission dynamics' is to divide a total population of N individuals into several classes analogous to the susceptible (S), infective (I), and recovered (R) sub-populations of conventional SIR epidemic models.[12,14,16,24] The dynamics of behavioural transmission are then characterised by how the sizes of these populations change with time. Our model of smoking dynamics follows in this tradition, and is in fact adapted from the four population approach of Sharomi and Gumel.[31] In our case, however, we use three populations, 'potential smokers' X, 'current smokers' Y, and 'former smokers' Z, omitting Sharomi and Gumel's fourth class of 'permanent quitters' (this does not imply that smokers cannot permanently cease smoking, it simply means that we assume any former smoker has some finite probability of relapse).[a] In this way, with total population $N = X + Y + Z$, we employ the following model

$$\frac{\mathrm{d}X}{\mathrm{d}\hat{t}} = \hat{\mu}N - \hat{\mu}X - \hat{\beta}X\left(\frac{Y}{N}\right), \tag{2.1a}$$

$$\frac{\mathrm{d}Y}{\mathrm{d}\hat{t}} = \hat{\beta}X\left(\frac{Y}{N}\right) + \hat{\alpha}Z - \hat{\gamma}Y - \hat{\mu}Y, \tag{2.1b}$$

$$\frac{\mathrm{d}Z}{\mathrm{d}\hat{t}} = \hat{\gamma}Y - \hat{\alpha}Z - \hat{\mu}Z, \tag{2.1c}$$

where $\hat{\mu}$ is the rate at which individuals both enter and exit the total population (comparable to birth and death-rates); $\hat{\beta}$ is the rate that potential smokers (X) take up smoking following contact with a current smoker (Y); $\hat{\gamma}$ is the proportion of current smokers (Y) who 'give up' smoking in time $\hat{t}$; and $\hat{\alpha}$ is the proportion of former smokers (Z) who 'relapse' to smoking at time $\hat{t}$. Notice that the $\hat{\beta}X(Y/N)$ term, which describes initial smoking uptake, has a linear proportionality to (Y/N), an effect reflecting the epidemiology convention that overall incidence of 'infection' is determined partly by the likelihood that a susceptible X interacts with an infective Y, and thus the density Y/N (the law of mass action[24]).

The rates themselves have been treated as single parameters; however, they should be understood as representing the combined effect of multiple mechanisms: those that act to increase the number of smokers by enhancing $\hat{\alpha}$ and $\hat{\beta}$, and suppressing $\hat{\gamma}$ (such as advertising, media presence, and celebrity endorsement); and those that act to reduce the number of smokers by suppressing $\hat{\alpha}$ and $\hat{\beta}$, and enhancing $\hat{\gamma}$ (such as health campaigns and governmental policy). Indeed, one of the main purposes of this article is to examine the effect of peer influence on these rates more explicitly by including incidence terms in both $\hat{\gamma}$ and $\hat{\alpha}$. Note that the use of identical entry and exit rates $\hat{\mu}$ is justified providing we assert a relatively young

[a]To prevent our notation becoming problem specific, we have chosen not to adopt that of Sharomi and Gumel, who used P for the class of potential smokers, S for the class of smokers, and Q for the class of former smokers ('quitters').[31] This choice should also help to avoid confusion between the *infective* class S in the smoking problem, and the *susceptible* class S in other SIR compartmental models (see, for example, references [12, 14, 16, 24]).

population with negligible death rate (cf. Sharomi and Gumel,[31] and others[19,23]). In this way, summation of equations (2.1) gives

$$\frac{\mathrm{d}N}{\mathrm{d}\hat{t}} = \frac{\mathrm{d}X}{\mathrm{d}\hat{t}} + \frac{\mathrm{d}Y}{\mathrm{d}\hat{t}} + \frac{\mathrm{d}Z}{\mathrm{d}\hat{t}} = 0, \tag{2.2}$$

i.e., the total population size N is constant. Consequently, after assuming constant $\hat{\mu}$, we may define a set of dimensionless parameters

$$x = \frac{X}{N}, \quad y = \frac{Y}{N}, \quad z = \frac{Z}{N}, \quad \text{so that} \quad x + y + z = 1, \tag{2.3a}$$

$$\alpha = \frac{\hat{\alpha}}{\hat{\mu}}, \quad \beta = \frac{\hat{\beta}}{\hat{\mu}}, \quad \gamma = \frac{\hat{\gamma}}{\hat{\mu}} \quad \text{and} \quad t = \hat{\mu}\hat{t}, \tag{2.3b}$$

and a normalised basic model constrained to two dimensions ($z = 1 - x - y$), *viz*

$$\frac{\mathrm{d}x}{\mathrm{d}t} = F(x, y) = (1 - x) - \beta xy, \tag{2.4a}$$

$$\frac{\mathrm{d}y}{\mathrm{d}t} = G(x, y) = \beta xy - (\gamma + 1)y + \alpha(1 - x - y), \tag{2.4b}$$

$$\frac{\mathrm{d}z}{\mathrm{d}t} = H(y, z) = \gamma y - (\alpha + 1)z, \tag{2.4c}$$

where the form of the final (redundant) equation has been included for completeness.

3. Basic Properties of the Model

Before proceeding to the generalised model, which includes terms to describe multiple peer influence effects in rates of cessation and relapse (see §4), we first consider its basic properties exclusive of the new effects. The relevant steady-states and their linear stability are summarised in §3.1 and §3.2 respectively.

3.1. *Existence of Steady-States*

In steady-state with parameter labels $x = x_0$, $y = y_0$ and $z = z_0$, we clearly require $F(x_0, y_0) = G(x_0, y_0) = H(y_0, z_0) = 0$. Solving equations (2.4) subject to this restriction we obtain the possible equilibrium solutions

$$\textbf{either:} \quad x_0 = 1, \qquad y_0 = 0 \qquad \text{and} \quad z_0 = 0, \tag{3.1}$$

$$\textbf{or:} \quad x_0 = \frac{1}{(\beta y_0 + 1)}, \quad y_0 = \frac{1}{\beta}\left[\frac{(1+\alpha)\beta}{(\alpha+\gamma+1)} - 1\right] \quad \text{and} \quad z_0 = \frac{\gamma y_0}{(\alpha+1)}. \tag{3.2}$$

Notice here that the first set of solutions, those in equations (3.1), define a 'smoking-free equilibrium' (S.F.E.) with $y_0 = 0$; while the second set, those in equations (3.2), correspond to a possible 'smoking-present equilibrium' (S.P.E.) with $y_0 > 0$ provided

$$R = \frac{(1+\alpha)\beta}{(1+\alpha+\gamma)} > 1 \quad \Leftrightarrow \quad \beta > 1 + \frac{\gamma}{(1+\alpha)} \quad \Rightarrow \quad \beta > 1, \tag{3.3}$$

where R is the *reproduction number*. Indeed, when this condition is satisfied, equations (3.2) give the physical solutions

$$(\beta y_0 + 1) = R \quad \Rightarrow \quad x_0 = \frac{1}{R} < 1, \quad \text{and} \quad y_0 = \frac{1}{\beta}(R-1) > 0. \tag{3.4}$$

The reproduction number determines how any given smoking 'epidemic' will spread: if R is less than unity, then no smoking-present equilibria exist and the 'infection' will die out (in this case the S.P.E. is unphysical since it would require $x_0 > 1$ and $y_0 < 0$); while if R is greater than unity then smoking-present equilibria are permitted, with larger R implying that a greater fraction of the population will be affected ($x \to 0$ as $R \to \infty$). As discussed in the introduction, therefore, one form of intervention to reduce the spread of smoking is to manipulate the rates such that R is kept as small as possible, i.e., by suppressing α and β, and enhancing γ.[b]

When we generalise the model to incorporate multiple peer influence mechanisms in §4, the rates of relapse α and cessation γ will be modified to include linear incidence terms, and thereby become functions of the population fractions x, y and z. As we shall see, this innovation will mean that equations (3.2) have the potential to specify multiple steady-states with $R \equiv R(x_0, y_0)$.

3.2. *Stability Exclusive of Generalised Peer Influence*

The stability of the basic model (excluding peer influence in α and γ) may be deduced from our later and more general analysis in §4, and for present purposes it is sufficient simply to summarise the main results. The stability of the smoking-free equilibrium is determined by the inequalities

$$\textbf{stable} \text{ S.F.E. when} \quad R \leq 1 \tag{3.5a}$$

$$\text{and } \textbf{unstable} \text{ S.F.E. for} \quad R > 1, \tag{3.5b}$$

meaning that for a smoking-present equilibrium to exist ($R > 1$), the S.F.E. must be unstable. If the S.P.E. does exist, then it is linearly asymptotically stable. A supplementary derivation of these results is included for reference in Appendix A.

4. Incorporating Generalised Peer Influence

The basic model of smoking dynamics described by equations (2.4) assumes that interactions between smokers and potential smokers can result in generation of new smokers through the recruitment incidence term βxy. We now generalise this idea to the rates of relapse and cessation in a similar way by introducing incidence terms into the constant rates α and γ; this seems reasonable given that:

- Former smokers (z) are more likely to revert to smoking following interactions with current smokers (y), i.e., lending αz some additional rate $\propto yz$.

[b]Notice that $\partial R/\partial\alpha = \gamma\beta/(1+\alpha+\gamma)^2 > 0$; the variations of R with β and γ are clear by definition.

- Both potential (x) and former (z) smokers (i.e., non-smokers) may well coerce current smokers (y) into 'giving-up', thereby introducing $\propto xy$ and $\propto yz$ incidence terms into γy.

On the basis of these assumptions, we therefore redefine α and γ such that

$$\alpha = a + \nu y \quad \text{and} \quad \gamma = c + \eta z + (\eta + \epsilon)x, \quad \text{with} \quad a, c, \nu, \eta, \epsilon \in \mathbb{R}_+, \tag{4.1}$$
$$\text{which gives} \quad \alpha z = az + \nu yz \quad \text{and} \quad \gamma y = cy + (\eta + \epsilon)xy + \eta yz,$$

where a and c are ambient rates of smoking relapse and cessation respectively; ν is the rate that former smokers relapse due to interactions with current smokers (y); η is the rate that current smokers 'give-up' smoking due to interactions with former smokers (z); and $(\eta + \epsilon)$ is the rate that current smokers 'give-up' smoking due to interactions with potential smokers. By taking $\epsilon \in \mathbb{R}_+$, we tacitly assume that individuals who have never smoked (potential smokers) will have greater coercive effect per capita on the rate at which current smokers stop smoking.[c] As before, these rates combine multiple effects: both those that are expected to increase the number of smokers (such as advertising and celebrity endorsement), and those that might reduce them (e.g., health campaigns and governmental policy). Indeed, with respect to the new peer influence terms, it seems natural that former smokers would be more likely to 'relapse' following contact with current smokers when smoking itself is given a 'positive profile'. And *vice versa*, current smokers will be more readily coerced into abstinence by non-smokers given broad societal intolerance to smoking. Note that α and γ retain ambient constant components, a and c respectively, since even without the effects of generalised peer influence, we expect some former smokers to 'relapse' (due to either addiction or societal effects, such as advertising) and some current smokers to 'quit' (in response to government campaigns, for example).

Incorporating the new peer influence rates of equation (4.1) into our basic model (2.4), we arrive at the augmented system

$$\frac{\mathrm{d}x}{\mathrm{d}t} = F(x, y) = (1 - x) - \beta xy, \tag{4.2a}$$
$$\frac{\mathrm{d}y}{\mathrm{d}t} = G(x, y) = \beta xy - (c + 1)y - (\eta + \epsilon)xy + (\nu - \eta)yz + a(1 - x - y), \tag{4.2b}$$
$$\frac{\mathrm{d}z}{\mathrm{d}t} = H(y, z) = cy + (\eta + \epsilon)xy - (\nu - \eta)yz - (a + 1)z. \tag{4.2c}$$

In the following sections we explore this modified model by demonstrating the existence of new steady-states and assessing their asymptotic stability. Before proceeding, however, it is worth making some general remarks about solutions: first, our assumption of constant total population is maintained, i.e., $x + y + z = 1$; second, equations (3.1) and (3.2) continue to define the smoking-free and smoking-present

[c]This assumption may be relaxed (i.e., $\epsilon < 0$ is also physically permitted), so long as incidence with potential smokers continues to enhance the cessation rate γ, that is, provided $(\eta + \epsilon) > 0$.

equilibria respectively; and third, for smoking-present equilibria (S.P.E.) to exist, we still require $R > 1$, and consequently—because α and γ remain positive—the inequality $\beta > 1$ (see equation (3.3)), though with the new peer influence terms $R \equiv R(x, y)$ is a function of the population densitite (see equation (4.5)). These points will be important when we come to establish whether-or-not algebraically derived steady-states are actually physically permitted. Notice that the basic model may be recovered from our augmented system, that is equations (4.2) reduce to equations (2.4), when ν, η, ϵ vanish and we have constant $\gamma = c$ and $\alpha = a$.

4.1. *Stability of the New Smoking Free Equilibrium*

With new definitions for α and γ it is important to reconsider the stability of the smoking-free equilibrium $(x_0, y_0) = (1, 0)$, and we now proceed to do so. The linear stability of a given equilibrium (x_0, y_0) may be determined in the usual way by considering the behaviour of perturbations to the steady-state values of the form $x_1 = \tilde{x}_1 e^{\lambda t}$ and $y_1 = \tilde{y}_1 e^{\lambda t}$, where $\tilde{x}_1$, $\tilde{y}_1$ and λ are constant, and $|\tilde{x}_1|, |\tilde{y}_1| \ll 1$.[8,24] Indeed, after setting $x = x_0 + x_1$, $y = y_0 + y_1$, Taylor expanding $F(x, y)$ and $G(x, y)$ in equations (4.2), and discarding non-linear terms, we have

$$\begin{pmatrix} \partial_x F & \partial_y F \\ \partial_x G & \partial_y G \end{pmatrix} \begin{pmatrix} x_1 \\ y_1 \end{pmatrix} = \lambda \begin{pmatrix} x_1 \\ y_1 \end{pmatrix}, \quad \text{where} \quad J(x_0, y_0) = \begin{pmatrix} \partial_x F & \partial_y F \\ \partial_x G & \partial_y G \end{pmatrix} \tag{4.3}$$

is the Jacobian matrix associated with model (4.2), and the partial derivatives $\partial_x F = \partial F / \partial x$ etc. are evaluated at $(x, y) = (x_0, y_0)$. In this way we see that the λ coefficients determining stability are the eigenvalues of $J(x_0, y_0)$, and may be found when non-trivial solutions to equation (4.3) exist, i.e., from the determinant

$$\begin{vmatrix} \partial_x F - \lambda & \partial_y F \\ \partial_x G & \partial_y G - \lambda \end{vmatrix} = 0. \tag{4.4}$$

In particular, these eigenvalues describe whether perturbations $\propto e^{\lambda t}$ on (x_0, y_0) either exponentially diverge from the steady-state (instability with $\lambda > 0$), or asymptotically converge back to equilibrium (asymptotic stability with $\lambda < 0$). In principle one can also derive inequalities governing asymptotic stability when $\lambda = 0$, a case to which we refer throughout as *marginal stability*, by examining second-order terms (or higher) in the Taylor expansion of model (4.2). However, stochasticity in realistic situations means the probability of the system exactly fulfilling marginally stable conditions will vanish, and consequently—while we do comment on which states *are* marginal—here we shall restrict ourselves to simply observing that a formal assessment of second-order stability requires a more detailed analysis of the non-linear terms. Note that marginal stability typically corresponds to cases where the linear stability of a steady-state changes polarity, or when two steady-states of opposing stability converge and annihilate (as with the 'tipping points' discussed in §4.5).[8]

In our augmented model $R \equiv R(x_0, y_0)$ is a function of both x_0 and y_0, that is,

$$R(x_0, y_0) = \frac{\big(1 + \alpha(y_0)\big)\beta}{\big(1 + \alpha(y_0) + \gamma(x_0, y_0)\big)} = \frac{(1 + a + \nu y_0)\beta}{\big(1 + a + c + \nu y_0 + \eta(1 - y_0) + \epsilon x_0\big)}, \tag{4.5}$$

(see equation (3.3), note that α and γ remain positive in the generalised system), so it is useful to define a *smoking-free reproduction number* R_0 such that

$$R_0 = R(1,0) = \frac{(1+a)\beta}{(1+a+c+\eta+\epsilon)} > 0, \tag{4.6}$$

i.e., $R(x_0, y_0)$ corresponding to the S.F.E. $(x_0, y_0) = (1, 0)$. Indeed, doing so means that the Jacobian matrix associated with the S.F.E. may be written

$$J(x_0,y_0) = J(1,0) = \begin{pmatrix} -1 & -\beta \\ (1-\varphi) & \beta(1-\varphi/R_0) \end{pmatrix}, \quad \text{where} \quad \varphi = (1+a), \tag{4.7}$$

which has eigenvalues λ given by solutions to the characteristic polynomial

$$\lambda^2 + \frac{1}{R_0}[R_0 + \beta(\varphi - 1) - \beta(R_0 - 1)]\lambda - \frac{\beta\varphi}{R_0}(R_0 - 1) = 0. \tag{4.8}$$

Several possibilities exist for the values of the coefficients in this quadratic, and we consider them in turn. Firstly, if $R_0 = 1$, then either

$$\lambda = 0 \quad \text{or} \quad \lambda = -(1 + a\beta), \tag{4.9}$$

in which case the linear stability of the S.F.E. is marginal. Secondly, when $R_0 > 1$, then it is possible for the set of square brackets in equation (4.8) to be zero, that is

$$R_0 + a\beta = \beta(R_0 - 1) \quad \Rightarrow \quad \lambda_\pm = \pm\left(\frac{\beta\varphi}{R_0}\right)^{1/2}(R_0 - 1)^{1/2}, \tag{4.10}$$

so that the S.F.E. is unstable by $\lambda_+ > 0$. [Note: $R_0 < 1$ is not possible here since $R_0 + a\beta = \beta(R_0 - 1)$ would then imply a contradiction.] In all other circumstances the eigenvalues of the Jacobian matrix defined in equation (4.7) are given by

$$\lambda_\pm = -\frac{1}{2R_0}[R_0 + a\beta - \beta(R_0 - 1)]\left\{1 \mp \left(1 + \frac{4\beta R_0\varphi(R_0-1)}{[R_0 + a\beta - \beta(R_0-1)]^2}\right)^{1/2}\right\}. \tag{4.11}$$

There are thus two final possibilities for the stability of the smoking-free equilibrium depending upon whether R_0 is greater than or less than unity. First, if $R_0 > 1$, then the term in curly brackets $\{1 \mp (\dots)^{1/2}\}$ changes sign with the polarity of the '$\mp$' symbol; in this case, the eigenvalues are of opposite sign, and the S.F.E. is unstable by either λ_+ or λ_-, whichever is positive. Second, if $R_0 < 1$, then the term in square brackets is positive and the real part of the term in curly brackets obeys $0 < \Re\{1 \mp (\dots)^{1/2}\} < 2$; thus, both $\Re\{\lambda_+\}$ and $\Re\{\lambda_-\}$ are negative and the S.F.E. is stable. Combining the above results, the linear stability of the smoking-free equilibrium may be summarised as:

$$\textbf{stable} \text{ S.F.E. when} \quad R_0 \le 1 \tag{4.12a}$$

$$\text{and } \textbf{unstable} \text{ S.F.E. for} \quad R_0 > 1, \tag{4.12b}$$

where marginal stability applies if $R_0 = 1$. These inequalities are consistent with those given in §3.2 and derived directly in Appendix A, that is, we recover our previous results when ν, η and ϵ vanish, for which $\alpha = a$, $\gamma = c$ and $R_0 = R$.

4.2. *Existence of New Smoking Present Equilibria*

The smoking-present equilibria $(x, y) = (x_0, y_0)$ defined by equations (3.2) exist whenever the value of the reproduction number R exceeds unity ($R > 1$); indeed, if this condition holds then equations (3.4) give (see §3):

$$x_0 = \frac{1}{R(x_0, y_0)}, \quad \text{and} \quad y_0 = \frac{1}{\beta}\big(R(x_0, y_0) - 1\big). \tag{4.13}$$

A useful approach to calculating the steady-states, therefore, is first to solve for $(R-1)$, thereby inferring possible solutions whenever $(R-1)$ is positive. Substituting the steady state values of equation (4.13) into equation (4.5) we find

$$(R-1)^2 - \Lambda(R-1) - \frac{\varphi\beta^2}{R_0\Delta}(R_0 - 1) = 0, \tag{4.14}$$

$$\text{with} \quad \Lambda = \left[(\beta - 1) - \frac{\beta}{\Delta}(1 + a + c)\right], \quad \text{and} \quad \Delta = (\nu - \eta). \tag{4.15}$$

Notice by equation (4.2b) that Δ describes the difference between: i) the rate ν at which former smokers (z) relapse following contact with current smokers (y); and ii) the rate η at which current smokers cease smoking due to contact with former smokers. In any given interaction between a current and a former smoker, it seems justifiable to assume that the former smoker is more likely to start smoking again than the current smoker is to stop; consequently, we take

$$\Delta > 0. \tag{4.16}$$

Solving the quadratic for $(R-1)$ in equation (4.14), we have

$$(R_\pm - 1) = \frac{1}{2}\Lambda\left\{1 \pm \left[1 + \frac{4\varphi\beta^2(R_0 - 1)}{\Delta R_0 \Lambda^2}\right]^{1/2}\right\}, \quad \text{for} \quad \Lambda \neq 0 \tag{4.17a}$$

$$\text{and} \quad (R_+ - 1) = \left[\frac{\varphi\beta^2(R_0 - 1)}{\Delta R_0}\right]^{1/2}, \quad \text{for} \quad \Lambda = 0. \tag{4.17b}$$

Notice that for equation (4.17a) to predict real, physical solutions (something we shall explore further in §4.5) we require

$$S = \left[1 + \frac{4\varphi\beta^2(R_0 - 1)}{\Delta R_0 \Lambda^2}\right] \geq 0 \tag{4.18}$$

where we call S the *realness parameter*. In equation (4.17b) the condition for real, physical solutions is $R_0 \geq 1$, which incidentally means that $S \geq 1$.

Assuming $S \geq 0$, equations (4.17) indicate that whether-or-not $(R-1)$ is positive—i.e., whether-or-not smoking-present equilibria obtain—depends on the signs of Λ and $(R_0 - 1)$; the possibilities may be summarised as follows:

- $\underline{\Lambda < 0:}$ For negative Λ the condition $(R_\pm - 1) > 0$ is only possible provided the term in curly brackets '$\{\dots\}$' in equation (4.17a) is also negative, which requires $R_0 > 1$. For these conditions only the S.P.E. corresponding to R_- is permitted, and converges on the marginal S.F.E. ($R_- \to R_0$) as $R_0 \to 1$.

- $\underline{\Lambda = 0}$: A single S.P.E. corresponding to R_+ is permitted provided $R_0 > 1$; this S.P.E. converges on the marginal S.F.E. ($R_+ \to R_0$) as $R_0 \to 1$.
- $\underline{\Lambda > 0}$: For positive Λ the S.P.E. corresponding to R_+ are always physically permitted, while those corresponding to R_- only obtain provided the square-bracketed term in equation (4.17a) is less than unity, i.e., $R_0 < 1$; for these conditions we have that $R_- \to R_0$ as $R_0 \to 1$.

As we shall see in the following section, it transpires that these S.P.E possibilities (either zero, one or two steady-states) may be tabulated in terms of the S.P.E. linear stability (see table 1). Before discussing them further, therefore, we must consider the Jacobian matrix associated with the new peer-influence model.

4.3. *Stability of the New Smoking Present Equilibria*

After some manipulation, the Jacobian matrix associated with the smoking-present equilibria (should they exist) may be written

$$J(x_0, y_0) = \begin{pmatrix} -R & -\beta/R \\ R\left[1 - \dfrac{\varphi}{R_0} - \dfrac{\Delta}{\beta^2}(R-1)\right] & \dfrac{\beta}{R}\left[1 - \varphi - \dfrac{\Delta}{\beta^2}R(R-1)\right] \end{pmatrix}, \tag{4.19}$$

As in §4.1, the linear stabilities of the equilibria are then determined by solving for the eigenvalues λ of $J(x_0, y_0)$, with $\lambda < 0$ and $\lambda > 0$ implying stability and instability respectively, *viz*

$$\lambda_\pm = -\frac{1}{2R\beta}[\beta R^2 + a\beta^2 + R(R-1)\Delta]\left\{1 \mp \sqrt{1 - \frac{8\beta R^2\Delta(R-1)[(R-1) - \frac{1}{2}\Lambda]}{[\beta R^2 + a\beta^2 + R(R-1)\Delta]^2}}\right\}. \tag{4.20}$$

For physical solutions we require $(R-1) > 0$, so the first square bracketed term here is positive, and the eigenvalues' signs depend only on whether the square root is greater than or less than unity. More specifically, if $[(R-1) - \frac{1}{2}\Lambda] < 0$, then the eigenvalues have opposite polarity with $\lambda_+ > 0$, while if $[(R-1) - \frac{1}{2}\Lambda] > 0$, then $\Re\{\lambda_\pm\} < 0$. Thus, the linear stability of the S.P.E. may be neatly summarised:

$$\textbf{stable} \text{ S.P.E. when} \quad [(R-1) - \tfrac{1}{2}\Lambda] \geq 0 \tag{4.21a}$$

$$\text{and } \textbf{unstable} \text{ S.P.E. for} \quad [(R-1) - \tfrac{1}{2}\Lambda] < 0, \tag{4.21b}$$

where the equality $[(R-1) - \frac{1}{2}\Lambda] = 0$ corresponds to marginal stability with $\lambda_- = 0$. However, by the steady-state solutions to R given in equation (4.17a) we find

$$[(R_\pm - 1) - \tfrac{1}{2}\Lambda] = \pm\frac{1}{2}\Lambda\left[1 + \frac{4\varphi\beta^2(R_0 - 1)}{\Delta R_0 \Lambda^2}\right]^{1/2} = \pm\frac{1}{2}\Lambda\sqrt{S}, \tag{4.22}$$

so that the stability of the possible S.P.E. $(x_0, y_0) = (x_\pm, y_\pm)$ are linked directly to the sign of Λ and the reproduction number (R_+ or R_-) with which they are associated. [Remember: equation (3.4) gives $x_\pm = x_0(R_\pm)$ and $y_\pm = y_0(R_\pm)$]. Indeed, by the inequalities (4.21), equation (4.22) means that the states (x_+, y_+) and

Sign of Λ	**Stability of S.F.E.**		
	Stable ($R_0 < 1$)	Marginal ($R_0 = 1$)	Unstable ($R_0 > 1$)
$\Lambda < 0$	no S.P.E. solution	$R_- = 1$ (Marginal)	$R_- > 1$ (Stable)
$\Lambda = 0$	no S.P.E. solution	$R_\pm = 1$ (Marginal)	$R_+ > 1$ (Stable)
$\Lambda > 0$	$R_+ > 1$ (Stable) $R_- > 1$ (Unstable)	$R_+ > 1$ (Stable) $R_- = 1$ (Marginal)	$R_+ > 1$ (Stable)

Table 1. The possible smoking-present equilibria (S.P.E.) tabulated in terms of their associated reproduction number R assuming $S \geq 0$, with their stability (in parenthesis) according to the sign of Λ and the linear stability of the smoking-free equilibrium (S.F.E.). Here 'no S.P.E.' means that no S.P.E. exist, i.e., either $R_\pm < 1$ or $\Re\{R_+\} = 0$, while single entries imply that the S.P.E. is unique. The pathological solutions $R = 1$ are identical to the S.F.E $(x_0, y_0) = (1, 0)$, and represent bifurcation points at which S.P.E. emerge (or disappear) following increases or decreases to R_0.

(x_-, y_-) have opposite stability. Naturally, whether S.P.E. actually exist depends on there being physical solutions to equation (4.17a), and—as we discussed in §4.2—this too is determined by the values of Λ and $(R_0 - 1)$. Consequently, it is possible to tabulate the steady-states in accordance with both their own linear stability *and* the stability of the smoking-free equilibrium. Demarcating solution space in this way, as we have done in table 1, demonstrates several key features:

- Stable S.F.E. and S.P.E. can coexist for the same set of parameters, that is, the system can exhibit bi-stability. This contrasts with results from the basic model, where the existence of the S.P.E. was predicated on the instability of the smoking-free equilibrium (see §3.2 and Appendix A).
- If the S.F.E. is stable ($R_0 < 1$), and if $\Lambda > 0$, then provided the realness parameter is positive ($S > 0$) two S.P.E. will exist (see §4.2 and §4.5), with $R_+ \leftrightarrow R_-$ as $S \to 0$. Conversely, if $S < 0$ when $R_0 < 1$ and $\Lambda > 0$, then solutions converge on a globally asymptotically stable S.F.E. (see §4.4).
- For $\Lambda \leq 0$ and $R_0 < 1$ no smoking-present equilibria exist. In this case, the smoking-free equilibrium is globally asymptotically stable (see §4.4).
- When the S.F.E. is unstable ($R_0 > 1$) then $S > 1 > 0$ is assured, and a single, stable smoking-present equilibrium exists; this is agrees with results from the basic model when generalised peer influence is excluded (see §3.2).
- For each condition based on the sign of Λ, the marginally stable S.F.E. ($R_0 = 1$) marks the bifurcation point for emergence or disappearance of smoking-present equilibria as R_0 is either increased of decreased.

Finally, observe (as expected) that equation (4.20) is consistent with our earlier statement asserting unconditional linear asymptotic stability of the S.P.E. when peer influence is excluded from α and γ (see §3.2). Indeed, taking $\nu, \eta, \epsilon \to 0$, such

that $\alpha = a$, $\gamma = c$, equation (4.20) becomes

$$\Re\{\lambda_\pm\} < -\frac{p_1}{2}(1 \mp 1) \leq 0, \quad \text{where} \quad p_1 = R + \frac{\alpha\beta}{R} > 0, \tag{4.23}$$

an expression which may be compared with equation (A.6) in Appendix A.

4.4. *Global Stability in Case of a Single Steady-State*

Before proceeding to our numerical and stochastic discussion of the new model (see §4.5, §4.6, and §5), it is worth reconsidering the stability of the smoking-free equilibrium when it is the only physical steady-state, i.e., for those situations when both $R_0 < 1$, and either $S < 0$ or $\Lambda \leq 0$, meaning no S.P.E. exist (see table 1). In these cases, inequalities (4.12) indicate that the S.F.E. is locally asymptotically stable; we now argue for the stronger condition that such stability is global.

Though model (4.2) describes the time dependence of three sub-populations, our constant total population condition $x + y + z = 1$, which asserts $x, y, z \in [0, 1]$, means that our system is effectively two dimensional in x and y, with a domain D of physically permitted solutions given by (see figure 1)

$$D = \{(x, y) \in \mathbb{R}^2_{\geq 0} : x + y \leq 1\}, \quad \text{with} \quad \mathbb{R}_{\geq 0} = \{x \in \mathbb{R} : x \geq 0\}. \tag{4.24}$$

It may be shown that D is invariant (see Appendix B), meaning that solutions stay within the domain. In addition, our system is plane autonomous, that is,

$$\frac{\mathrm{d}x}{\mathrm{d}t} \equiv \dot{x} = F(x, y) \quad \text{and} \quad \frac{\mathrm{d}y}{\mathrm{d}t} \equiv \dot{y} = G(x, y) \tag{4.25}$$

with $F(x, y)$ and $G(x, y)$ as single valued, continuous Lipschitz functions[d] on D (see equations (4.2)), so that by Picard's Theorem solutions with initial conditions $\big(x(0), y(0)\big) = (\tilde{x}, \tilde{y})$ trace out unique trajectories $\big(x(t), y(t)\big)$ in the phase-plane. Notice also that the nulcline $y = (1 - x)/\beta x$ associated with $\dot{x} = 0$ divides D into two regions: one for which $\dot{x} > 0$, and another for which $\dot{x} < 0$ (see figure 1). These features may be used to argue for global stability as follows.

Since we are assuming conditions permitting only one steady-state, excepting the S.F.E. located at $(1, 0)$ there can be no points on $\dot{x} = 0$ at which $\dot{y} = 0$, meaning that the sign of $\dot{y}$ cannot change on $\dot{x} = 0$. Consequently, because $\dot{y}$ is negative at the intercept of $y = (1 - x)$ and $y = (1 - x)/\beta x$, that is,

$$\dot{y} = -\left(\frac{(\beta - 1)}{\beta}\right)\left(c + \frac{(\eta + \epsilon)}{\beta}\right) < 0 \quad \text{for} \quad (x, y) = \left(\tfrac{1}{\beta}, \tfrac{(\beta-1)}{\beta}\right), \tag{4.26}$$

we have $\dot{y} < 0$ for all trajectories crossing $\dot{x} = 0$. These trajectories traverse $\dot{x} = 0$ vertically downwards and, because $y = (1 - x)/\beta x$ is a monotonically decreasing

[d]The following Lipschitz conditions may be shown to hold for $(x, u) \in D$ and $(x, v) \in D$:

$$|F(x, u) - F(x, v)| \leq \beta|u - v|, \quad |G(x, u) - G(x, v)| \leq (1 + a + c + \eta + \epsilon + \beta + 3\Delta)|u - v|.$$

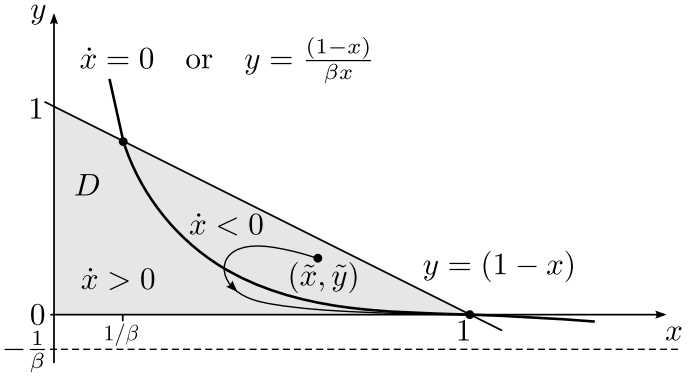

Fig. 1. Phase-space sketch indicating how an arbitrary trajectory (curve with arrow) starting at $(\tilde{x}, \tilde{y})$ converges on $(1, 0)$ provided the S.F.E. is the only physical steady-state, i.e., $R_0 < 1$ and either $\Lambda \leq 0$ or $S < 0$. The nulcline corresponding to $\dot{x} = 0$, namely $y = (1 - x)/\beta x$, divides D into two regions of $\dot{x}$ with opposing sign (cf. figure 7).

function of x, take solutions $\big(x(t), y(t)\big)$ from the regions of D where $\dot{x} < 0$ to the region where $\dot{x} > 0$; trajectories traversing D in the opposite sense are forbidden.

Now suppose our initial conditions are such that $(\tilde{x}, \tilde{y})$ is in the region of D for which $\dot{x} < 0$; because $\dot{x}$ is negative, the solution trajectory points in the direction of decreasing x towards the curve $\dot{x} = 0$ where $\dot{y} < 0$, and thence into the region for which $\dot{x} > 0$ (see figure 1). Further, by our argument in the preceding paragraph, solutions beginning in or passing through this region (for which $x(t)$ is monotonically increasing, $\dot{x} > 0$) cannot cross $\dot{x} = 0$, and are therefore subject to the conditions

$$0 \leq y(t) < \min\left\{(1 - x(t)), \frac{(1 - x(t))}{\beta x(t)}\right\}, \quad \dot{x}(t) > 0, \quad \text{and} \quad x(t) \to 1. \qquad (4.27)$$

Hence, when the smoking-free equilibrium is the only permitted steady-state its globally asymptotic stability is assured, that is, $(x, y) \to (1, 0)$ (see figure 1).

4.5. *Preliminary Numerical Discussion*

Our main discussion of systemic parameter sensitivity forms part of the stochastic analysis in the following section (§5.2); nevertheless, it is instructive at this stage to consider a few numerical features of the model within the purely deterministic framework, especially variations in the number of steady-state solutions. To this end we focus on the impact of the new peer influence terms in ϵ, η and ν, adopting nominal values for the overall rates similar to those considered by Sharomi and Gumel,[31] specifically $\alpha \sim \beta \sim \gamma \sim 6$. Naturally, our peer influence assumptions mean that α and γ are functions of x, y and z, and for this reason the values for a, ν, c, η and ϵ will be chosen to ensure that $\alpha \sim \beta \sim \gamma \sim 6$ is maintained for characteristic population densities based on recently compiled smoking statistics for the Northeast of England,[15] i.e., $(x, y, z) \approx (0.4, 0.3, 0.3)$. Of particular interest

is the region of parameter space for which $\Lambda > 0$ and $R_0 < 1$, since in this case the system exhibits bi-stability (see table 1); we shall set the ambient rates to $a = c = 0.5$, such that these conditions on Λ and R_0 are satisfied, and consider each incidence parameter, ϵ, η and ν, in turn (§4.5.1, §4.5.2 and §4.5.3 respectively).

4.5.1. *Scanning over ϵ*

We begin by taking $[\nu, \eta] = [11, 5]$ and scan over $\epsilon \in (0, 5)$, since with $(x, y, z) \approx (0.4, 0.3, 0.3)$ this choice gives $\alpha = c + \nu y \sim 6$ and $\gamma = \eta z + (\eta + \epsilon)x \sim 6$ as required. As we discuss below, because these values yield $\Lambda = 3 > 0$, the change in the number of steady-states with ϵ which we plot in figure 2 may be understood by referring to the final row of table 1.

For $\epsilon < 2$ we have $R_0 > 1$, implying an unstable S.F.E. and—by equation (4.17a) and inequlity (4.21a)—a *single* stable S.P.E. given by $R_+ > 1$ (the second solution $R_- < 1$ is non-physical); this is the steady-state (x_+, y_+) corresponding to the third column (final row) in table 1. At $\epsilon = 2$ we find $R_0 = R_- = 1$, so the stability of the S.F.E. becomes marginal and heralds the emergence of a new S.P.E. given by (x_-, y_-), while the S.P.E. (x_+, y_+) remains stable; the conditions in this case correspond to those in the second column (final row) of table 1.

Now suppose that ϵ is increased such that $\epsilon > 2$, but remains less than some critical value ϵ_c. With $\epsilon > 2$ we find $R_0 < 1$, so the S.F.E. is now stable; but we also have $R_- > 1$, implying the full emergence of a second *unstable* S.P.E. (x_-, y_-) to complement the *stable* solution (x_+, y_+). These conditions equate to those in the first column (final row) of table 1. However, notice from figure 2 that as ϵ tends towards ϵ_c (≈ 4.3 for our chosen parameters), the two S.P.E. solutions meet at a single equilibrium $R_+ = R_-$. As may be seen from equations (4.17a) and (4.18), such convergence reflects the dependence of $(R_\pm - 1) = \frac{1}{2}\Lambda\left\{1 \pm S^{1/2}\right\}$ on the value of the 'realness parameter' S: as ϵ approaches the critical value ϵ_c, the magnitude of S tends towards $S(\epsilon_c) = 0$. This solution is particular important because it represents the point at which the S.P.E. determined by $R_\pm$ become complex, i.e., $S(\epsilon > \epsilon_c) < 0$, and therefore forbidden; for these conditions ($S < 0$) the only physical solution is the *stable* smoking-free equilibrium given by $R_0 < 1$. [**Note:** The stability of the S.P.E. at $\epsilon = \epsilon_c$ is marginal, anticipating an approaching shift in the equilibrium solution.]

4.5.2. *Scanning over η*

We scan over $\eta \in (0, 5)$ in a similar way to that described above, with the other parameters fixed at $[\nu, \epsilon] = [11, 5]$. This time Λ is a function of our scanning variable η; however, the inequality $\Lambda(\eta) > 0$ holds over the entire range, so the conditions correspond to those in the final row of table 1 as before. In fact, the results in this case are qualitatively similar to those listed in §4.5.1 (compare figures 2 and 3): first, for $\eta < 2$, we have $R_0 > 1$, $R_- < 1$ and $R_+ > 1$, implying both an

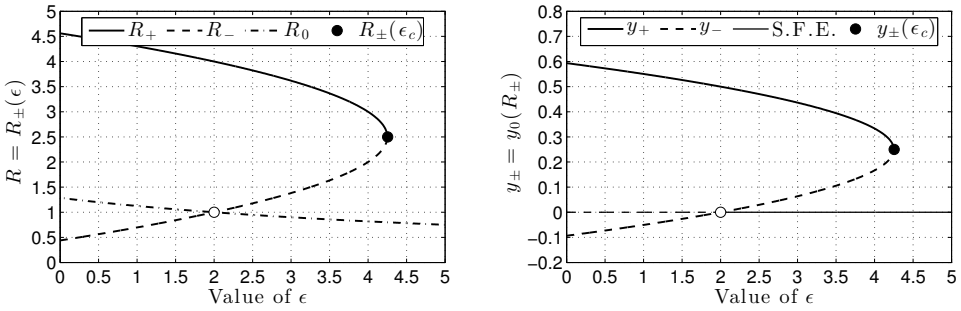

Fig. 2. **Left:** Solutions for the steady-state reproduction numbers R_0 (S.F.E.) and $R_\pm$ (S.P.E.) as a function of ϵ at fixed $[\nu, \eta] = [11, 5]$. The critical value ϵ_c, when $R_+ = R_-$, represents a possible smoking 'tipping point' beyond which the S.P.E. become complex, and therefore unphysical (see §4.6 and right-hand plot). **Right:** Steady-state 'current smoker' population densities $y_\pm$ corresponding to the $R_\pm$ (S.P.E.) reproduction numbers ('thick' curves), with the S.F.E. $y_0 = 0$ indicated by the 'thin' curves (both solid and dashed). The point at which the S.F.E. is only marginally stable (white circle) is also shown. Here the solid curves are linearly stable states, while the dashed curves are either linearly unstable, or (as is the case when $y_- < 0$) unphysical.

unstable S.F.E., and a *single* stable S.P.E. (third column); second, for $\eta = 2$, we have $R_0 = R_- = 1$ and $R_+ > 1$, implying a marginally stable S.F.E., and a *single* stable S.P.E. (second column); third, for $2 < \eta < \eta_c$, where η_c is some critical value, we have $R_0 < 1$, $R_- > 1$ and $R_+ > 1$, implying a *stable* S.F.E., an *unstable* S.P.E., and a *stable* S.P.E. respectiveley (first column) . At the critical value η_c (≈ 4.6 for our chosen parameters), the two S.P.E. merge to a marginally stable steady-state, beyond which ($\eta > \eta_c$) solutions become complex and therefore unphysical.

4.5.3. *Scanning over ν*

Finally we consider $\nu \in (10, 15)$ with $[\eta, \epsilon] = [5, 5]$, a range ensuring $\Delta = (\nu - \eta) > 0$ as required by inequality (4.16). In this case $R_0 = 0.75$ is constant (R_0 is independent on ν), and, since $\Lambda > 0$, all solutions correspond to those of the first column (final row) of table 1; indeed, for ν greater than the its critical value ν_c (the value at which which $R_+ = R_-$), both stable and unstable S.P.E. obtain. However, in a similar fashion to that described above, decreasing ν below ν_c destroys the S.P.E. as the realness parameter S goes negative and solutions become complex (see figure 3). Notice here that the transition from three to one steady-state solutions occurs by *reducing* ν, reflecting its status as the peer influence term which encourages smoking *relapse*; this contrasts with the shift to a single S.F.E. for *increasing* ϵ and η, since these terms describe coercion of smokers (by non-smokers) to abstain.

4.6. *'Tipping Points' in Societal Smoking Dynamics*

As discussed in section 4.4, when the S.F.E. is the only physical steady state ($R_0 < 1$, and either $S < 0$ or $\Lambda \leq 0$) it is also globally asymptotically stable, so that the

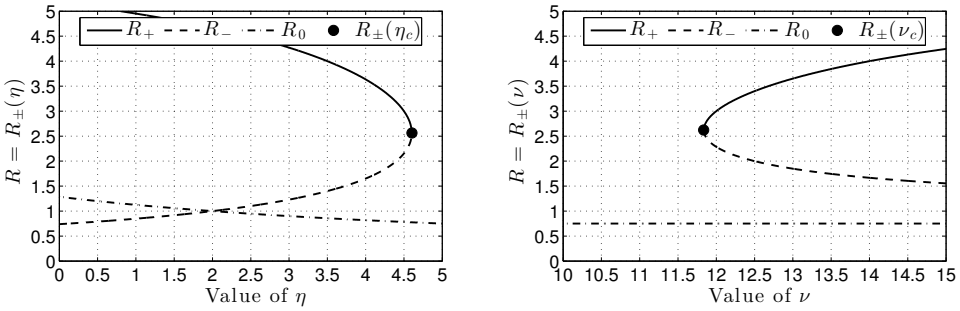

Fig. 3. Solutions for the steady-state reproduction numbers R_0 (S.F.E.) and $R_\pm$ (S.P.E.) as a function of both η at fixed $[\nu, \epsilon] = [11, 5]$ (left, cf. figure 2), and ν at fixed $[\eta, \epsilon] = [5, 5]$ (right). The critical values η_c and ν_c are those for which $R_+ = R_-$, and represent possible smoking 'tipping points' beyond which the S.P.E. become complex, and therefore unphysical (see §4.6).

existence of critical values ν_c, ϵ_c and η_c indicates possible discontinuous 'tipping points' in societal smoking dynamics.[e]

To see this consider both the left and right-hand plots in figure 2, starting at $\epsilon = 1$, for which only the S.P.E. associated with R_+ is stable and the density of smokers given by equation (4.13) exceeds half the population, i.e., $y_+ = [R_+(\epsilon)-1]/\beta \approx 0.55$. If we increase ϵ to its critical value ($\epsilon_c \approx 4.3$ for our chosen parameters), the S.P.E. remains stable until the point $y_+ = [R_+(\epsilon_c) - 1]/\beta \approx 0.25$ when approximately a quarter of the population are smoking; however, further increase to ϵ will destroy the S.P.E. (see §4.5.1), and the system must reconfigure to the remaining steady-state, i.e., the smoking-free equilibrium (see §4.4 and figure 4). In this way, the critical value becomes a societal 'tipping point': if ϵ_c is reached, then even very small increments to the success with which potential smokers x encourage or coerce smokers into abstinence (the term in ϵ) lead to total smoking cessation (S.F.E.). The role of such critical values in determining system hysteresis, and their presence in global parameter space, are discussed further in the following subsections.

4.6.1. *System Hysteresis*

It is in the immediate stages following societal 'tipping' to S.F.E. that the hysteresis effect becomes important. As shown in figure 2, simply reducing ϵ to its value prior to 'tipping' will not revert the system to a smoking-present equilibrium, because while the S.P.E. associated with $R_\pm(\epsilon_c)$ is *unstable*, the S.F.E. given by $R_0(\epsilon_c) < 1$ is *stable*. In fact, if we assume that solutions *always* converge to a steady-state, then as ϵ is reduced, we expect the system to remain at the smoking-free equilibrium until $\epsilon = 2$ is reached; beyond this point the S.F.E. becomes unstable ($R_0 > 1$), and the system 'tips' back to the stable smoking-present equilibrium associated with R_+

[e]This feature is especially evident in the dependance of S.P.E. on ϵ (and η), in which case—as we discuss in §4.6.1—the system has the potential to exhibit hysteresis cycling.

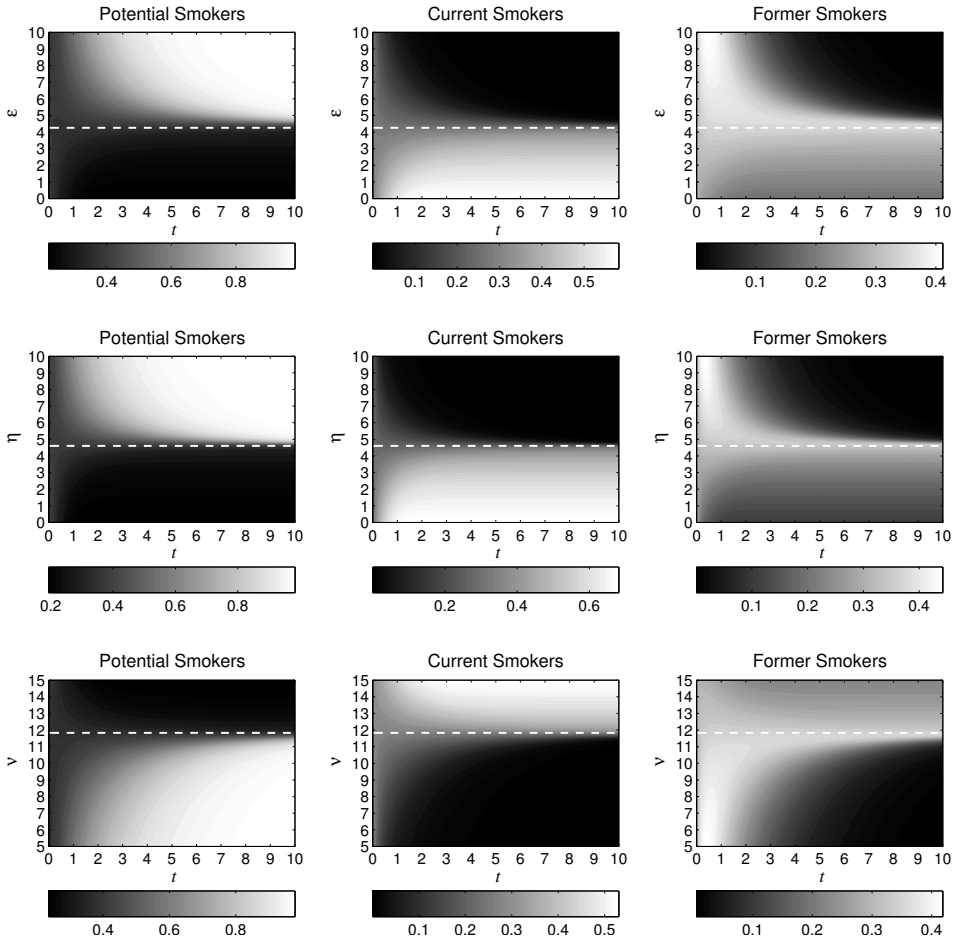

Fig. 4. Numerical solution of the peer-influence model for $\beta = 6$, $a = c = 0.5$, and a range of ϵ (top row with $[\nu, \eta] = [11, 5]$, see §4.5.1), η (middle row with $[\nu, \epsilon] = [11, 5]$, see §4.5.2) and ν (bottom row with $[\eta, \epsilon] = [5, 5]$, see §4.5.3). Here we have taken initial values for the population densities $(x_0, y_0, z_0) = (0.4, 0.3, 0.3)$, consistent with current data from the Northeast of England (see the introduction to §4.5), while the greyscale colourbars indicate the size of each subpopulation at a given time t. The (white) dashed lines show the critical values—here $(\epsilon_c, \eta_c, \nu_c) \approx (4.3, 4.6, 12)$—for which the realness parameter S changes sign, and represent societal smoking 'tipping points'.

(see figure 2). Naturally, once returned to the S.P.E. given by $R_+(\epsilon = 2)$, the system will remain stable until ϵ is *increased* to its critical value ϵ, thereby completing the cycle. Given the potential importance of this kind of hysteresis cycle, formal proof of non-linear stability in the neighbourhood of the S.P.E would form an important part of any future study (cf. our discussion of global S.F.E. stability when $R_0 < 1$, and either $S < 0$ or $\Lambda \leq 0$ in §4.4).

Interestingly, because R_0 is not a function of ν, no hysteresis cycle follows vari-

ations in the peer influence to relapse. If the system 'tips' from a stable S.P.E. in this case (by reducing ν below its critical value η_c, see §4.5.2), then no change to ν is capable of destabilising the S.F.E. to which it reconfigures, a result which may be encouraging to those seeking absolute suppression of cigarette smoking. Nevertheless, as we shall discuss in the following subsection, R_0 can be pushed above unity by modifying the parameters on which it *does* depend, thereby rendering the S.F.E. unstable and a return to the smoking-present equilibrium (which always exist when $R_0 > 1$, see equation (4.17a)).

4.6.2. *General Comments on 'Global Tipping Points'*

So far our discussion of 'tipping points' in the generalised peer influence model has been restricted to describing how the model behaves as a single variable is changed and the others are held constant. Naturally, in the real world one would expect parameters to change simultaneously, and for this reason it is appropriate to make some general remarks about what might be called 'global tipping points', those which occur when more than one parameter is varied.

First, notice that systemic 'tipping' from an S.P.E. to S.F.E. requires conditions for which $R_0 < 1$, $\Lambda > 0$ and $S > 0$, because the system must exhibit bi-stability if it is to switch from one stable state to another. Indeed, since discontinuous 'tipping points' essentially represent parameter-space transitions from an S.P.E. location within table 1 (namely the bi-stable state in the first column, final row) to a non-physical location completely outside the table, they can *only* occur when S changes sign from positive to negative. Transitions within the table to positions marked 'no S.P.E. solution' do not represent 'tipping points': either because the steady-state would first pass smoothly through an equilibrium with $R_\pm = 1$, identical to the marginal S.F.E. (as is the case with transitions from the second column); or because solutions become non-physical (S goes negative) and 'leave' the table before such a transition can occur (as is the case when Λ changes sign).[f]

Given these conditions for discontinuous transitions from a stable S.P.E. to a stable S.F.E., we can make the following general comment about 'tipping points' in six-dimensional global parameter space $V = \{(\beta, a, c, \nu, \eta, \epsilon) \in \mathbb{R}^6_+ : (\nu - \eta) > 0\}$: assuming that the system is initially at some stable smoking-present equilibrium (S.P.E.), any path $P(t) = P\big(\beta(t), a(t), c(t), \nu(t), \eta(t), \epsilon(t)\big)$ through the sub-space $V_s = \{(\beta, a, c, \nu, \eta, \epsilon) \in V : \Lambda(\beta, a, c, \nu, \eta) > 0, R_0(\beta, a, c, \eta, \epsilon) < 1\}$ which crosses the surface $S(\beta, a, c, \nu, \eta, \epsilon) = 0$ from a region where $S > 0$ into $S < 0$ will take the system through a discontinuous 'tipping point' to a stable smoking-free equilibrium.

In fact, we can go further by giving limits on the population densities $(x_\pm, y_\pm)$

[f] A transition from the bi-stable state ($R_0 < 1$, $\Lambda > 0$ and $S > 0$) to the 'no S.P.E. solution' given by $R_0 < 1$ and $\Lambda \leq 0$ requires the value of Λ to pass through zero; however, since $S(\Lambda, R_0 < 1) \to -\infty$ as $\Lambda \to 0^+$, the solution would 'tip' by S changing sign before such a transition could occur.

corresponding to the marginally stable S.P.E. at the 'tipping surface' $S = 0$. Since

$$R_{\pm}(S=0) = \frac{\Lambda+2}{2} \quad \text{and} \quad 0 < \Lambda = \left[(\beta-1) - \frac{\beta}{\Delta}(1+a+c)\right] < (\beta-1), \quad (4.28)$$

with $x_{\pm} = 1/R_{\pm}$ and $y_{\pm} = (R_{\pm}-1)/\beta$ (see equation (4.13)), we have that

$$\frac{2}{\beta+1} < \frac{2}{\Lambda+2} = x_{\pm} < 1, \quad \text{and} \quad 0 < y_{\pm} = \frac{\Lambda}{2\beta} < \frac{1}{2}\left(1 - \frac{1}{\beta}\right) < \frac{1}{2}; \quad (4.29)$$

so the density of smokers (y) must be less than half the total population before societal tipping to a smoking-free equilibrium can occur.

5. Sensitivity Analysis and Stochastic Modelling

By definition, a deterministic model does not incorporate uncertainty, and for a given set of initial conditions, it will always return the same output. Consequently, one can extract a number of properties—such as those listed in the previous sections—which yield valuable information about system behaviour. Nevertheless, no matter how sophisticated a deterministic approach might be, it can never completely represent the system that is being modelled: issues such as uncertainty derived from randomness, lack of information, parameter sensitivity, and incompleteness of the model itself, are all tacitly excluded. Since we are interested in using our augmented system (4.2) to model societal smoking dynamics in the real world, it is now essential that such uncertainty be addressed.

In the following sections we investigate systemic uncertainty of model (4.2) in two ways. First (§5.1), we assess parameter sensitivity using Sobol's variance-based approach, which can be adapted for both deterministic and stochastic models (see references [25, 32]); we want to compute the main effects and interactions through time of each model parameter, thereby investigating both their impact on overall output, and temporal changes in their effects, especially in the region of possible 'tipping points'. Second (§5.2), we examine the impact of random fluctuations (noise) on model (4.2) by constructing an analogous stochastic representation. As with our deterministic sensitivity analysis (§5.1), the stochastic approach is also assessed in terms of both parameter uncertainty and sensitivity (§5.3 and §5.4 respectively).

5.1. *Sensitivity of the Deterministic Model*

Any model can be seen as a simulator that takes a set of inputs and return a set of outputs. Here our simulator is given by the augmented system of differential equations (4.2), with input space formed by the variables β, a, c, ν, η, ϵ and starting points $x(0)$, $y(0)$, $z(0)$, and a dynamic output space formed by the population sizes $x(t)$, $y(t)$ and $z(t)$ at each time $t > 0$. Notice that with $x(t) + y(t) + z(t) = 1$ our input space is 8-dimensional, while our output space is two-dimensional. In reference [32], the main effect index for a given input variable ϕ is defined by the average of the output variance of its contribution (as determined by varying ϕ

alone, holding the other input subspaces fixed) normalised to the model's total variance. Letting $P_i(t)$, $i = 1, \ldots, 8$ represent the input space parameters at time t, and $K(t) = \{x(t), y(t), z(t)\}$ be the model output at time t, the main effect $S(t)_{ij}$ of an input parameter P_i on the output K_j $(j = 1, \ldots, 3)$ at time t, is thus

$$S_{ij}(t) = \frac{\mathrm{Var}_{P_i}\left[E_{-i}(K_j(t)|P_i(t))\right]}{\mathrm{Var}(K_j(t))}. \tag{5.1}$$

Here the integral on the numerator of each index can become computationally expensive as the number of input parameters and the number of time steps required for accuracy increases. Nevertheless, since paths in the deterministic model vary smoothly through time, this is not a serious problem, and to estimate the main effect indices $S(t)_{ij}$ we use a Monte Carlo method based on a 16-dimensional Latin hypercube design with a correlation-based criterion. The indices show convergence with around 1000 sample surfaces, where each surface contains 500 time samples in the interval $[0, 10]$; each index is calculated at each time step for all 8 input variables, and independently for each output variable. These results are displayed in figure 5; note that we omit the higher-order interaction indices since their values are negligible for all values of t.

As we would expect from a robust model, the start points $x(0)$, $y(0)$ account for a fairly small amount of the model's variability. We observe that the population of potential smokers responds mostly to the initial smoking incidence rate β. The population of smokers responds strongly both to the ambient rates of relapse a and cessation c, and moderately to: the initial incidence β; the rate of relapse due to interactions with current smokers ν; and the rate of cessation due to interactions with former smokers η. Finally, of all the parameters, the population of former smokers seems most affected through time by the ambient rate of cessation c; however, initial uptake β and relapse a have some effect too. This analysis also indicates that our new parameters, those used to generalise the effect of peer influence, are relevant, and account for a significant part of the output's variability.

Our above discussion has shown how these three subpopulations respond to initial conditions and model parameters in an ideal environment with constant population size, constant parameters, and no uncertainty. From §4.6.2, we can see that changes in β seem to be the most relevant when investigating tipping points; indeed, our model's behaviour on the 'tipping surface' indicates that once a transition from an S.P.E. to stable S.F.E. ($R_0 < 1$) occurs, substantial changes to either β, a or c are nedeed to force $R_0 > 1$, destabilise the S.F.E., and change states again. This is consistent with the indices in figure 5, since the two main subpopulations, potential smokers and current smokers, are most sensitive to these three parameters (a, c, β).

Having discussed model sensitivity to changes in initial input parameters (which are then held constant over the duration of simulation), we must also consider how the system behaves when these parameters and populations are subject to continual uncertainty; to this end, we now turn our attention to developing a three-population stochastic analogue of the deterministic model (4.2).

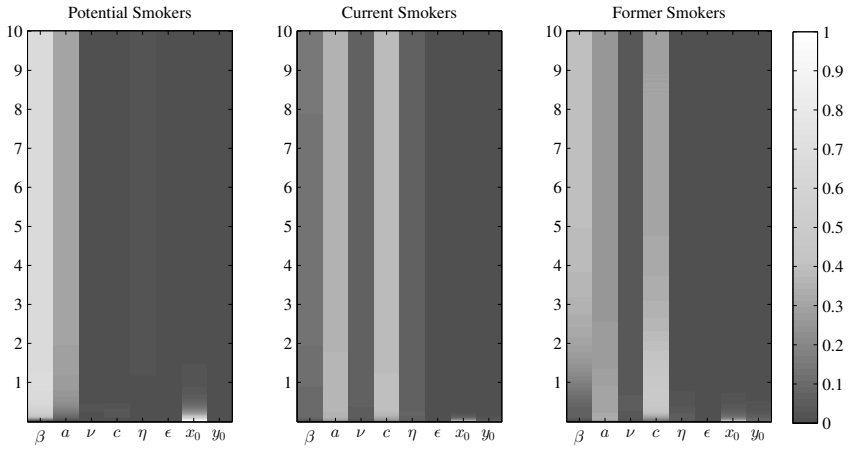

Fig. 5. Main effects by population for the parameters β, a, c, η, ϵ, ν (abscissa axis), and starting points $x(0)$, $y(0)$, and time $t \in [0, 10]$ (ordinate axis). The effects are calculated using Sobol's decomposition, and standardised by the model's total variance; the higher a parameter's effect at a given time, the more sensitive the corresponding population will be to small variations in said parameter. As expected for a robust model, its sensitivity to variations in the subpopulation start points is low relative to the main parameters; this indicates that regardless of the model's initial state, in most cases it is possible to implement policies to change the final population distribution.

5.2. *Stochastic Analogue of the Deterministic Model*

We now consider a stochastic analogue of the deterministic system with generalised peer influence (model (4.2)). Let $\{K(t) : t \in T\}$ be a stochastic process (where $K = (x, y, z)$ is a vector representing the populations of potential (x), current (y), and former (z) smokers, and T is some time interval), and define $\mathbf{b} : \mathbb{R}^3 \to \mathbb{R}^3$, with $b_1 = F(x, y)$, $b_2 = G(x, y)$ and $b_3 = H(y, z)$ as in equations (4.2). We then define the corresponding Wiener process for the three-population deteministic model as

$$\mathrm{d}K(t) = \mathbf{b}\big(K(t)\big)\mathrm{d}t + B\mathrm{d}W(t) \tag{5.2}$$

where $\mathrm{d}W(t)/\mathrm{d}t$ represents three-dimensional white noise (i.e., the time derivative of a Wiener process), $B\sqrt{\mathrm{d}t} = \sqrt{V}$, and V is a positive definite covariance matrix. Further defining the expected value $E\big(\mathrm{d}K(t)\big) = b\big(K(t)\big)\mathrm{d}t$, we say that the covariance matrix V is given by

$$\begin{aligned} \mathrm{Var}\big((\mathrm{d}K(t)\big) &= E\big(\mathrm{d}K(t)(\mathrm{d}K(t))'\big) - E\big(\mathrm{d}K(t))E(\mathrm{d}(K(t))\big)' \\ &\approx E\big(\mathrm{d}K(t)(\mathrm{d}K(t))'\big),\ E\big(\mathrm{d}K(t))E(\mathrm{d}(K(t))\big)' \in \mathcal{O}\big((\mathrm{d}t)^2\big). \end{aligned} \tag{5.3}$$

Rewriting the system of equations in the three population model, we have

$$\begin{aligned} \mathrm{d}X(t) &= F(X, Y)\mathrm{d}t + B_{11}\mathrm{d}W_1 + B_{12}\mathrm{d}W_2 + B_{13}\mathrm{d}W_3 \\ \mathrm{d}Y(t) &= G(X, Y)\mathrm{d}t + B_{21}\mathrm{d}W_1 + B_{22}\mathrm{d}W_2 + B_{23}\mathrm{d}W_3 \\ \mathrm{d}Z(t) &= H(Y, Z)\mathrm{d}t + B_{31}\mathrm{d}W_1 + B_{32}\mathrm{d}W_2 + B_{33}\mathrm{d}W_3 \end{aligned} \tag{5.4}$$

where W_1, W_2 and W_3 are three independent Wiener processes.

This is an Îto stochastic process and satisfies the Existence and Uniqueness Theorems (see Kloeden & Platen [17]); moreover, when solutions for the deterministic system exist, the trajectories of these stochastic differential equations converge uniformly on a closed time interval to the deterministic solutions. Therefore, in near-ideal conditions of low noise and small parameter variability, the mean distribution of this stochastic process is expected to converge to the deterministic paths. This only means that the underlying behaviour of the stochastic model would be *similar* to the deterministic; stochastic paths will most likely differ from the ideal case when subject to any form of noise.

Figure 6, gives an example of this stochastic system using starting points based on statistics for the Northeast of England,[15] that is, $(x, y, z) \approx (0.4, 0.3, 0.3)$: the solid and dashed lines show the underlying deterministic model and a sample stochastic path respectively, while the patches represent 95% quantiles for each population. Here the parameters and start points are identical (and fixed) for all simulations, and B is a randomly generated positive-definite matrix. Notice that the overall mean path is not affected, and is indistinguishable from the deterministic path after 1000 samples; however, it is clear that sample paths can be fairly different from the mean path, and even if the mean process appears to have reached stability, this does not necessarily correspond to stability of the sample path.

5.3. *Sensitivity of the Stochastic Model*

In this section we investigate the sensitivity of the stochastic model using the same method we applied to our deterministic system in §5.1 above. First we analyse the case where B is diagonal, with entries restricted to the interval $[0, 1]$ (it would be unrealistic to accept noise levels higher than the population size). Since for the stochastic model we need to consider sensitivity in the diagonal of B, we now have an 11-dimensional input space defined by the six rates β, a, c, η, ν, ϵ, the two starting points $x(0)$, $y(0)$, and the three matrix elements B_{11}, B_{22}, B_{33}. We use a quasi-Monte Carlo method and a 22-dimensional (22D) Latin hypercube sample to estimate the main effects for each input at the times $t \in [0, 10]$. Due to the increased number of input parameters and the variability caused by the stochasticity of the model, the time interval $\Delta t = 0.002$ is finely sampled, and convergence for all parameters appears after around 10^5 samples in our 22D latin hypercube.

The response of the three populations to the main parameters and start points is similar to the effects in the deterministic model; the effect of start points is slightly higher for small values of t but is quite small when compared to the effects of β, a and c. The second variational parameter B_{22} is the only one to have a significant effect in any of the three subpopulations; its effect is higher in the populations of potential smokers x and former smokers z, which is consistent with the fact that the population of current smokers y directly affects the other two populations. The variational parameters show that oscillations in the populations of potential and

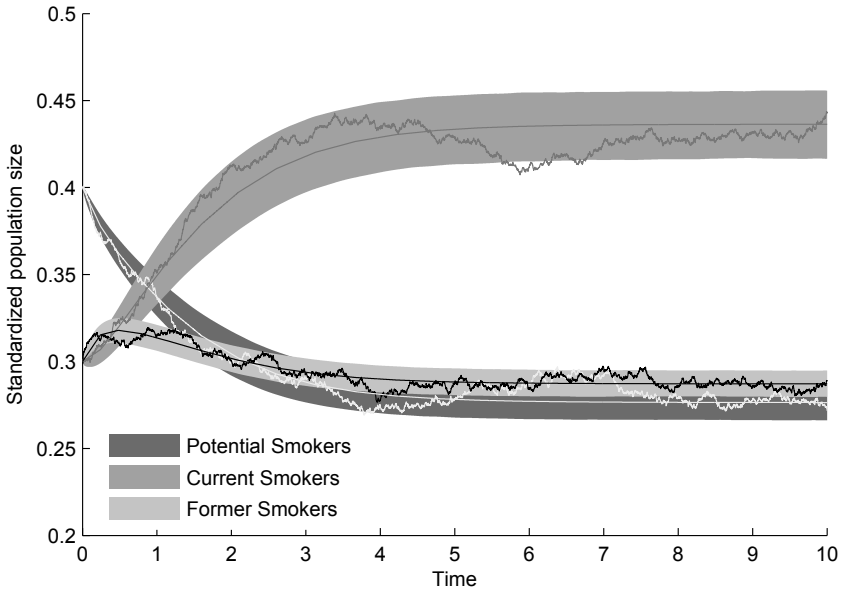

Fig. 6. Example of the stochastic system in Equation 5.4. The 'smooth' lines correspond to the deterministic model, while the 'noisy' lines represent a sample stochastic path, and the patches are the 95% quartiles for each population. The asymptotic values are $(x, y, z) \approx (0.28, 0.44, 0.29)$.

former smokers, unlike the population of current smokers, do not affect the overall stability of the model, but significant changes to the population of smokers can lead to a change in state.

Now we analyse the case where B is a symmetric positive-definite covariance matrix with entries in the interval $[-1, 1]$. In this situation our input space consists of the six main model parameters β, a, c, η, ν, ϵ, the two start points $x(0)$ and $y(0)$, and six covariance parameters. Given the dimensionality of such a problem, and its new correlation structure, estimating the main effect parameters becomes more expensive. To achieve satisfactory convergence for the main effects, we keep the time sampling interval at $\Delta t = 0.002$ and generate 10^8 samples in a 28-dimensional Latin hypercube. Since we have to guarantee that the matrix B is positive definite, we test for positiveness in each sample, resampling if the condition is not met.

The sensitivity profile of this model is still similar to the original parameters in the deterministic model, but the effects of the background relapse a and cessation rates c is reduced in the population of potential smokers, and increased in the populations of current smokers and former smokers. In the population of current smokers, the effect of parameters other than a and c is negligible, while in the other two populations, the effect of the correlation parameters is more evident. The subpopulation of potential smokers shows higher effects for the parameters linked to the

population of current smokers B_{12}, B_{22} and B_{23}, implying that interactions between the population of non-smokers $(x + z)$ and smokers (y) are the most important.

The main effects of the correlation parameters on the population of former smokers is almost the same for all parameters, with B_{12} and B_{33} slightly higher than the remaining four. The increased significance of B_{12} in this population (z) seems to reflect part of the effect of the initial uptake β and cessation c rates, since a substantial increase in both these rates would lead to an increase in this population. The response of the population of non-smokers $(x + z)$ to these correlation parameters might also indicate the need to modify the model to include more parameters describing interactions between the three groups, or add a temporal variability to some of the parameters that are assumed constant. Overall, from the three sensitivity analysis discussed here, we see that the population of current smokers y is the most robust and least sensitive to fluctuations, while from the remaining two, the population of potential smokers x is most responsive to changes in the modelling parameters, and the population of former smokers z most volatile when the stochasticity is incorporated.

5.4. *Uncertainty of the Stochastic Model*

We are studying a three-population stochastic model with a 14-dimensional parameter space comprising the six parameters β, a, c, η, ν, ϵ from the generalised deterministic model (4.2), two start points $x(0)$ and $y(0)$, and six correlation parameters (elements of B). Despite having a low-dimensional problem, prior information and expert judgements about the rates that we are investigating are scarce, meaning that a high-level of uncertainty and possible ambiguity exists regarding interpretation of model outputs.[26] The sensitivity analyses conducted above (§5.1 and §5.3), indicate to which parameters the model is more robust; we know that those parameters to which the model is most sensitive—e.g., rates of initial uptake β and cessation c—are also those most likely to induce high variability in the final outputs.

We also analysed parameter interactions, noting them to be fairly small; however, this does not imply that they are uncorrelated. In fact, they are likely to be correlated through interactions with one or more subpopulations, suggesting that in future works we should investigate parameters as functions of time and subpopulations. The datasets currently available are small and simplistic, providing temporal data on the three population sizes, but little information about contact rates, or motivation for initial uptake or cessation.[15] Moreover, it is known that some people who categorise themselves as "casual smokers" deny being "smokers" when asked; given that the class of potential smokers x could be seen as the most influential category, and the class of former smokers z the most volatile, such behaviour could considerably affect the uncertainty linked to these two populations, especially given that our model portrays the current smoker class y as the most robust. So, regardless of how unrealistic a three-population model might initially appear, investing in a more complex model would not necessarily result in improved predictive capacity

until the uncertainty in simple models such as ours can be understood; indeed many variables related to social behaviour are unmeasurable or unobservable.

6. Conclusion

We have developed a new compartmental model for describing the transmission of socially determined behaviours when generalised 'peer influence' terms act between each of the subpopulations, and discussed it in the context of societal smoking dynamics. Both deterministic (§4) and stochastic (§5) aspects have been considered: in the former, we derived general results about system dynamics, such as the number of steady-states and the nature of their asymptotic stability; while in the latter, we examined aspects of uncertainty that are essential to interpreting model output for application to real-world situations.

In the deterministic analysis (§4), we demonstrated that new peer influence terms in rates of relapse and cessation result in markedly new behaviour (when compared to a basic model for which peer influence is assumed in rates of initial uptake only). In particular, we found that the inclusion of generalised peer influence allows for additional equilibria (§4.2), system bi-stability (§4.1, §4.3, §4.4 and §4.5), and the introduction of both 'tipping point' dynamics and hysteresis (§4.6). These results contrast with the basic model, where for a given set of model parameters only a single stable steady-state is permitted (see §3). Such features may be of considerable interest to both health practitioners and policy makers: for example, the existence of societal 'tipping points' suggest that (for some conditions) sustained changes to system parameters can eventually lead to dramatic system shifts; while the presence of hysteresis means that such changes might persist in the long-term. The new aspects are also significant from a purely modelling perspective: the fact that relatively small changes to the underlying system (introduction of new incidence terms) can induce such novel behaviour, raises important questions about structural stability of the compartmental approach.[4,9,19,22,23,28,31,34]

The sensitivity analyses and stochastic simulations of our generalised model in §5 showed that the three sub-population classes are responsive to the new parameters, justifying the introduction of multiple peer influence terms. However, while we have been able to initialise our simulations with known population densities (those relevant to the Northeast of England[15]) the difficulty in obtaining reliable information about other system parameters means that further research is needed to fully understand model uncertainty. In future, we need to investigate the impact of new interaction terms and non-linear incidence (either as functional or stochastic processes), since this would help to account for changes in behaviour, both through time, and with population distribution. Indeed, topics such as non-linear incidence are known to have important consequences for compartmental modelling in epidemiology,[13,18,20] and so are also likely to be relevant to social dynamics.

More generally, there exist a number of fundamental questions concerning mathematical descriptions of social behaviour. Certainly, another way of viewing the

smoking dynamics problem modelled here is as a complex system, one in which the decisions of individual agents are likely to vary heterogeneously, with a range of *nonlinearly additive*[2] interactions. Our compartmental method neglects some of these aspects by treating the system on a macroscopic scale assuming heterogeneity to be averaged out as a mean-field. Nevertheless, one can go deeper into the microscopic structure by taking a statistical approach and using game theory to model the output of individual interactions,[3,6,30] while the impact of heterogeneity can be investigated directly by studying games on graphs.[29] It would be interesting to consider further the relationship of the macroscopic compartmental method adopted here to—or indeed emergence from—smaller scale multi-agent systems (see, for example, Bellomo *et al.*[1,2,3] and references therein).

Nevertheless, while our present model is based on assumptions that are only likely to fit a specific age group or region at any given time, more sophisticated social elements can be included at the macroscopic scale by adding new compartmental groups, and allowing them to mix and interact. The next step, therefore, would be to incorporate age and gender structure to the model, and indeed entirely new classes (such as 'casual' and 'chain' smokers) with different vital dynamics (for a discussion of non-linear age dependent population dynamics see G. F. Webb [33]); spatial heterogeneity could also be addressed, either through use of patch models,[21] or systems of partial differential equations.[24] However, as our present study has shown, if such developments are to have practical consequences for the work of health practitioners, then more comprehensive data is needed than that currently available, especially regarding rates of smoking uptake and cessation; ideally, therefore, future modelling activities should be undertaken in conjunction with new empirical studies.

Appendix A. Stability of the Basic Model

Although our approach is inspired by Sharomi and Gumel,[31] the fact that we use three populations rather than four means that the stability of our basic model does not directly follow from their original paper.[31] For completeness, therefore, we now include a direct stability analysis of the S.F.E. and S.P.E. when multiple peer influence is excluded (§A.1 and §A.2 below). Note that the stability conditions found here represent limiting cases with which to compare the results derived from our more general peer influence model in §4.

A.1. *Smoking Free Equilibrium*

We analyse the stability of the smoking-free equilibrium $(x_0, y_0, z_0) = (1, 0, 0)$ using the 'next generation method' described by Sharomi and Gumel.[7,31] Linearising equations (2.4b) and (2.4c) about $y_0 = z_0 = 0$ by taking $y = y_1 e^{\lambda t}$ and $z = z_1 e^{\lambda t}$, with $y_1, z_1 \in \mathbb{R}_+$ and λ constant, we find

$$\left(\underline{\underline{\mathbf{A}}} - \underline{\underline{\mathbf{B}}}\right) \cdot \mathbf{v} = \lambda \mathbf{v}, \quad \text{where} \quad \mathbf{v} = \begin{pmatrix} y_1 \\ z_1 \end{pmatrix}, \tag{A.1}$$

and the matrices $\underline{\underline{\mathbf{A}}}$ and $\underline{\underline{\mathbf{B}}}$ are defined such that $\underline{\underline{\mathbf{B}}}$ is an M-matrix, i.e., has non-negative diagonal elements and non-positive off diagonal elements, *viz*

$$\underline{\underline{\mathbf{A}}} = \begin{pmatrix} \beta & 0 \\ 0 & 0 \end{pmatrix} \quad \text{and} \quad \underline{\underline{\mathbf{B}}} = \begin{pmatrix} (\gamma+1) & -\alpha \\ -\gamma & (\alpha+1) \end{pmatrix}. \tag{A.2}$$

Since $y, z \propto \exp(\lambda t)$, the stability of the S.F.E. depends on the signs of the eigenvalues λ of $(\underline{\underline{\mathbf{A}}} - \underline{\underline{\mathbf{B}}})$. Fortunately, by defining $\underline{\underline{\mathbf{A}}}$ and $\underline{\underline{\mathbf{B}}}$ as we have done, these may be readily determined[7,31]; indeed, in this case the next generation method states that providing the spectral width ρ_s of the matrix $\underline{\underline{\mathbf{A}}} \cdot \underline{\underline{\mathbf{B}}}^{-1}$ exceeds unity, then there exists *at least* one positive eigenvalue $\lambda > 0$, otherwise all $\lambda \leq 0$. More specifically, if $\rho_s(\underline{\underline{\mathbf{A}}} \cdot \underline{\underline{\mathbf{B}}}^{-1}) = \sup\{||\lambda_k||\} > 1$, where λ_k are the $k = 1, 2$ eigenvalues of $(\underline{\underline{\mathbf{A}}} \cdot \underline{\underline{\mathbf{B}}}^{-1})$, then the S.F.E. given by $(x, y, z) = (1, 0, 0)$ is unstable. In this way, it is possible to demonstrate $\rho_s(\underline{\underline{\mathbf{A}}} \cdot \underline{\underline{\mathbf{B}}}^{-1}) = R$ and thus

$$\textbf{stable} \text{ S.F.E. when} \quad R \leq 1 \tag{A.3a}$$

$$\text{and } \textbf{unstable} \text{ S.F.E. for} \quad R > 1, \tag{A.3b}$$

where the equality applies to the marginally stable state for which equations (3.1) and (3.2) yeild identical solutions (cf. inequalities (4.12) in §4.1). Consequently, for the S.P.E. to exist, i.e., $R > 1$, the S.F.E. must be unstable.

A.2. *Smoking Present Equilibrium*

For $R > 1$ and constant α and γ, the smoking-present equilibrium (x_0, y_0) given by equations (3.2)—or identically by equations (3.4)—is unique and defines a Jacobian matrix associated with equations (2.4) of the form

$$J(x_0, y_0) = \begin{pmatrix} \partial_x F & \partial_y F \\ \partial_x G & \partial_y G \end{pmatrix} = \begin{pmatrix} -R & -\beta/R \\ R - (\alpha+1) & -\alpha\beta/R \end{pmatrix}. \tag{A.4}$$

The eigenvalues of $J(x_0, y_0)$ are thus found by solving the characteristic polynomial

$$\lambda^2 + p_1\lambda + p_2 = 0, \quad \text{where} \quad p_1 = R + \frac{\alpha\beta}{R} \quad \text{and} \quad p_2 = \beta(\alpha+1)\frac{(R-1)}{R}. \tag{A.5}$$

Since both coefficients of this quadratic are positive (we require $R > 1$ for an S.P.E.), the real parts of the possible eigenvalues are accordingly negative:

$$\Re\{\lambda_\pm\} < -\frac{p_1}{2}(1 \mp 1). \tag{A.6}$$

Hence, the smoking-present equilibrium is always locally asymptotically stable.

Appendix B. Closure of Solution Space

Our argument for global stability of the S.F.E. when it is the only steady-state (see §4.4) assumes that the system stays within the domain D of physical solutions

$$D = \{(x, y) \in \mathbb{R}^2_{\geq 0} : x + y \leq 1\}, \quad \text{with} \quad \mathbb{R}_{\geq 0} = \{x \in \mathbb{R} : x \geq 0\}, \tag{B.1}$$

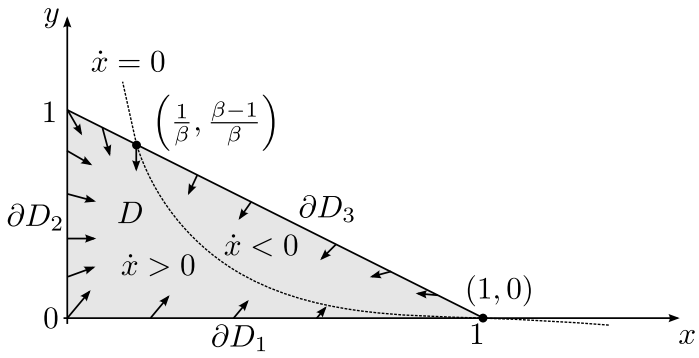

Fig. 7. Qualitative sketch showing trajectories starting from the domain boundary (arrows) crossing ∂D into D. Note the intersections of the nulcline $\dot{x} = 0$ (dashed) with $y = (1-x)$, and the division of D into regions where $\dot{x} > 0$ and $\dot{x} < 0$ (cf. figure 1).

i.e., that D is invariant. Recalling that the trajectory at a given point (x, y) is given by the direction of the phase-space velocity vector $(\dot{x}, \dot{y})$, where

$$\dot{x} = F(x, y) = (1 - x) - \beta xy, \tag{B.2a}$$

$$\dot{y} = G(x, y) = \big(\beta - (\eta + \epsilon)\big)xy - (c + 1)y + \big((\nu - \eta)y + a\big)(1 - x - y), \tag{B.2b}$$

(see model 4.2), the gradient of a trajectory in phase-space is given by

$$\left(\frac{\mathrm{d}y}{\mathrm{d}x}\right)_{x,y} = \frac{\dot{y}(x, y)}{\dot{x}(x, y)}, \quad \text{for} \quad \dot{x} \neq 0. \tag{B.3}$$

Hence, closure can be established after demonstrated how—with the exception the *critical* point $(x, y) = (1, 0)$ corresponding to smoking-free equilibrium—the trajectory of a solution $\big(x(t), y(t)\big)$ starting from a point $\big(x(0), y(0)\big) = \big(\tilde{x}, \tilde{y}\big)$ on the boundary ∂D of the domain will cross it (i.e., is non-parallel to ∂D) in such a way as to take solutions further into D. We proceed with such an approach in the following sections, dividing $\partial D \backslash \{(1, 0)\}$ into three segments such that

$$\partial D = \partial D_1 \cup \partial D_2 \cup \partial D_3 \cup \{(1, 0)\}, \tag{B.4}$$

where ∂D_1, ∂D_2, and ∂D_3 are defined

$$\partial D_1 = \{(x, y) \in \mathbb{R}^2 : 0 < x < 1, y = 0\}, \tag{B.5a}$$

$$\partial D_2 = \{(x, y) \in \mathbb{R}^2 : 0 \leq y \leq 1, x = 0\}, \tag{B.5b}$$

$$\partial D_3 = \{(x, y) \in \mathbb{R}^2_+ : (x + y) = 1\}. \tag{B.5c}$$

respectively (see figure 7), and represent those parts of ∂D excluding $\{(1, 0)\}$ which coincide with either the coordinate axis or the line $y = (1 - x)$.

B.1. *Boundary on the x-axis*

For $(\tilde{x}, \tilde{y}) \in \partial D_1$ we have $\tilde{y} = 0$ and $\tilde{x} \in (0, 1)$, and thus

$$\dot{x} = (1 - \tilde{x}) > 0, \quad \text{and} \quad \dot{y} = a(1 - \tilde{x}) > 0, \quad \Rightarrow \quad \left(\frac{\mathrm{d}y}{\mathrm{d}x}\right)_{\tilde{x},\tilde{y}} = a > 0. \tag{B.6}$$

Since the gradient of this trajectory is positive (and therefore none parallel to ∂D_1, which has zero gradient) with $\dot{x}, \dot{y} > 0$, solutions starting from $(\tilde{x}, \tilde{y})$ cross the boundary deeper into D (see figure 7). Notice that the magnitude $\sqrt{\dot{x}^2 + \dot{y}^2}$ of the phase-space velocity on ∂D_1 obeys

$$\lim_{\tilde{x}\to 1^-} \left(\sqrt{\dot{x}^2 + \dot{y}^2}\right) = \lim_{\tilde{x}\to 1^-} \left((1 - \tilde{x})\sqrt{1 + a^2}\right) = 0, \tag{B.7}$$

consistent with our critical point $(x, y) = (1, 0)$ as the smoking-free equilibrium.

B.2. *Boundary on the y-axis*

For $(\tilde{x}, \tilde{y}) \in \partial D_2$ we have $\tilde{x} = 0$ and $\tilde{y} \in [0, 1]$, and thus

$$\dot{x} = 1 > 0, \quad \text{and} \quad \dot{y} = a - (1 + a + c - \Delta)\tilde{y} - \Delta\tilde{y}^2, \quad \Rightarrow \quad \left(\frac{\mathrm{d}y}{\mathrm{d}x}\right)_{\tilde{x},\tilde{y}} = \dot{y}. \tag{B.8}$$

Positive $\dot{x}$ here means that trajectories starting from $(\tilde{x}, \tilde{y}) \in \partial D_2 \backslash \{(0, 0), (0, 1)\}$ cross ∂D into the domain D; however, it remains for us to show that this is also true for the limiting points of ∂D_2, namely $(0, 0)$ and $(0, 1)$. Observing

$$\lim_{\tilde{y}\to 0^+} \left(\frac{\mathrm{d}y}{\mathrm{d}x}\right)_{\tilde{x},\tilde{y}} = a > 0 \quad \text{and} \quad \lim_{\tilde{y}\to 1^-} \left(\frac{\mathrm{d}y}{\mathrm{d}x}\right)_{\tilde{x},\tilde{y}} = -(1 + c) < -1, \tag{B.9}$$

we see that at $(0, 0)$ the gradient is greater than that of the boundary segment ∂D_1 (which has a gradient of 0), while at $(0, 1)$ the gradient is less than that of the boundary segment ∂D_3 (which has a gradient of -1); hence, solutions starting from either point will be carried deeper into the domain (see figure 7).

The limits (B.9) indicate that the trajectory gradient on ∂D_2 must change sign on $\tilde{y} \in (0, 1)$, and by equation (B.8) this occurs when $\dot{y} = 0$. Indeed, solving $\dot{y} = 0$ subject to the condition $\tilde{y} > 0$ we find

$$\tilde{y} = \tilde{y}_h = \frac{1}{2\Delta}\left\{\big(\Delta - (1 + a + c)\big) + \sqrt{\big(\Delta - (1 + a + c)\big)^2 + 4a\Delta}\right\} > 0, \tag{B.10}$$

as the point on ∂D_2 where the trajectory is horizontal. [**Note:** Since for any a and c we have that $\tilde{y}_h$ is a monotonically increasing function of Δ, with both $\tilde{y}_h \to 1$ as $\Delta \to \infty^-$, and $\tilde{y}_h \to \big(a/(1 + a + c)\big)$ as $\Delta \to 0^+$, this gives $\tilde{y}_h \in (0, 1)$ as required (these limits are consistent with results in §B.1 above and §B.3 below).]

B.3. *Boundary on the Curve* $y = (1 - x)$

For $(\tilde{x}, \tilde{y}) \in \partial D_3$ we have $y = (1 - x)$ and $\tilde{x} \in (0, 1)$, and thus

$$\dot{x} = (1 - \beta\tilde{x})(1 - \tilde{x}), \quad \text{and} \quad \dot{y} = (1 - \tilde{x})\big((1 - \beta\tilde{x}) - (c + (\eta + \epsilon)\tilde{x})\big). \tag{B.11}$$

At the point $\left(\frac{1}{\beta}, \frac{\beta-1}{\beta}\right)$, this means that $\dot{x} = 0$ and $\dot{y} < 0$, and the trajectory crosses ∂D_3 vertically downwards, further into D (see figure 7). Elsewhere we have

$$\left(\frac{\mathrm{d}y}{\mathrm{d}x}\right)_{\tilde{x},\tilde{y}} = \begin{cases} -\left(1 + \dfrac{c + (\eta + \epsilon)\tilde{x}}{(1 - \beta\tilde{x})}\right) < -1, & \text{for} \quad \tilde{x} < \dfrac{1}{\beta} \\ -\left(1 + \dfrac{c + (\eta + \epsilon)\tilde{x}}{(1 - \beta\tilde{x})}\right) > -1, & \text{for} \quad \tilde{x} > \dfrac{1}{\beta}, \end{cases} \tag{B.12}$$

so none of these trajectories are parallel to ∂D_3 (which has gradient -1), and must therefore also traverse it: that they do so in the sense of taking solutions deeper into D is guaranteed given that $\dot{x} > 0$ for $\tilde{x} < \frac{1}{\beta}$, and $\dot{x} < 0$ for $\tilde{x} > \frac{1}{\beta}$, and

$$\lim_{\tilde{x}\to 0^+} \left(\frac{\mathrm{d}y}{\mathrm{d}x}\right)_{\tilde{x},\tilde{y}} = -(1 + c) < 0 \tag{B.13}$$

(this is consistent with the gradient at $(0, 1)$ found in §B.2). Furthermore, as we saw in §B.1, the magnitude $\sqrt{\dot{x}^2 + \dot{y}^2}$ of the phase-space velocity on ∂D_3 obeys

$$\lim_{\tilde{x}\to 1^-} \left(\sqrt{\dot{x}^2 + \dot{y}^2}\right) = 0, \tag{B.14}$$

as expected given our smoking-free equilibrium $(x, y) = (1, 0)$.

Acknowledgments

This work was supported by a Leverhulme Trust Grant (Tipping Points Project, Institute of Hazard, Risk, and Resilience, University of Durham).

References

1. N. Bellomo, H. Berestycki, F. Brezzi and J. P. Nadal, Mathematics and Complexity in Life and Human Sciences, *Math. Models Methods Appl. Sci.* **20** (2010) 1391–1395.
2. N. Bellomo and F. Brezzi, Mathematics and Complexity in Biological Sciences, *Math. Models Methods Appl. Sci.* **21** (2011) 819–824.
3. N. Bellomo and F. Brezzi, Mathematics and Complexity of Multi-Particle Systems, *Math. Models Methods Appl. Sci.* **22** (2012) 1103001.
4. N. Bellomo and L. Preziosi, *Modelling Mathematical Methods and Scientific Computation*, (CRC Press, Boca Raton, 1995).
5. D. Bernoulli and S. Blower, An attempt at a new analysis of the mortality caused by smallpox and of the advantages of inoculation to prevent it, *Rev. Med. Virol.* **14** (2004) 275–288.
6. M. A. Chakra and A. Traulsen, Evolutionary Dynamics of Strategic Behavior in a Collective-Risk Dilemma, *PLoS Comput. Biol.*, **8** (2012) e1002652.
7. P. van den Driessche and J. Watmough, Reproduction numbers and sub-threshold endemic equilibria for compartmental models of disease transmission, *Math. Biosci.* **180** (2002) 29–48.

8. P. Glendinning, *Stability, instability and chaos : an introduction to the theory of nonlinear differential equations* (Cambridge University Press, 1994).
9. B. Gonzáleza *et al.*, Am I too fat? Bulimia as an Epidemic, *J. Math. Psychol.* **47** (2003) 515–526.
10. M. B. Gordon, J. P. Nadal, D. Phan and V. Semeshenko, Discrete Choices Under Social Influence: Generic Properties, *Math. Models Methods Appl. Sci.* **19** (2009) 1441–1481.
11. Z. Harakeh and W. A. M. Vollebergh, The impact of active and passive peer influence on young adult smoking: An experimental study, *Drug Alcohol Depend.* **121** (2012) 220–223.
12. H. W. Hethcote, Qualitative analyses of communicable disease models, *Math. Biosci.* **28** (1976) 335–356.
13. H. W. Hethcote and P. van den Driessche, Some epidemiological models with nonlinear incidence, *J. Math. Biol.* **29** (1991) 271–287.
14. H. W. Hethcote, The mathematics of infectious diseases, *SIAM Review* **42** (2000) 599–653.
15. *Data from the integrated household survey : Smoking prevalence among adults aged 18+ by region and local authority*, U. K. Department of Health, Aug 2012, URL `http://www.lho.org.uk/viewResource.aspx?id=16678` (Accessed on 15$^{\text{th}}$ Aug 2012).
16. W. O. Kermack and A. G. Mc Kendrick, A contribution to the mathematical theory of epidemics, *Proc. R. Soc. A* **115** (1927) 700–721.
17. P. E. Kloeden and E. Platen, *Numerical Solutions of Stochastic Differential Equations* (Springer, 1992).
18. A. Korobeinikov and P. K. Maini, Non-linear incidence and stability of infectious disease models, *Math. Med. Biol.* **22** (2005) 113–128
19. A. Lahrouz *et al.*, Deterministic and stochastic stability of a mathematical model of smoking, *Statist. Probab. Lett.* **81** (2011) 1276–1284.
20. W. Liu, H. W. Hethcote, and S. A. Levin, Dynamical behavior of epidemiological models with nonlinear incidence rates, *J. Math. Biol.* **25** (1987) 359–380.
21. A. L. Lloyd and R. M. May, Spatial Heterogeneity in Epidemic Models, *J. theor. Biol.* **179** (1996) 1–11.
22. G. Mulone and B. Straughan, A note on heroin epidemics, *Math. Biosci.* **218** (2009) 138–141.
23. G. Mulone and B. Straughan, Modeling binge drinking, *Int. J. Biomath.* **5** (2012) 1250005.
24. J. D. Murray. *Mathematical Biology: I. An Introduction* (Springer, 3rd Edition, 2002).
25. J. Oakley and A. O'Hagan, Probabilistic sensitivity analysis of complex models: a Bayesian approach, *J. Roy. Statist. Soc. Ser. B* **66** (2004) 751–769.
26. J. T.Oden and S. Prudhomme, Control of modeling error in calibration and validation processes for predictive stochastic models, *Int. J. Numer. Meth. Engng* **87** (2011) 262–272.
27. Public Health Research Consortium (PHRC), United Kingdom. *A Review of Young People and Smoking in England : Final Report.* (May, 2009).
28. G. P. Samanta, Dynamic behaviour for a nonautonomous heroin epidemic model with time delay, *J. Appl. Math. & Computing* **35** (2011) 161–178.
29. F. C. Santos, J. M. Pacheco, and T. Lenaerts, Evolutionary dynamics of social dilemmas in structured heterogeneous populations, *Proc. Natl. Acad. Sci. USA* **103** (2006) 3490–3494.
30. F. C. Santos, V. V. Vasconcelos, M. D. Santos, P. N. B. Neves, and J. M. Pacheco, Evolutionary Dynamics of Climate Change Under Collective-Risk Dilemmas, *Math. Models Methods Appl. Sci.* **22** (2012) 1140004.

31. O. Sharomi and A.B. Gumel, Curtailing smoking dynamics: A mathematical modeling approach, *Appl. Math. Comput.* **195** (2008) 475–499.
32. I. Sobol, Sensitivity estimates for nonlinear mathematical models, *Mathematical Modeling and Computational Experiment* **1** (1993) 407–414.
33. G. F. Webb. *Theory of Nonlinear Age-Dependent Population Dynamics* (Marcel Dekker, New York, 1985).
34. E. White and C. Comiskey, Heroin epidemics, treatment and ODE modelling, *Math. Biosci.* **208** (2007) 312–324.
35. World Health Organisation. WHO report on the global tobacco epidemic, 2011: warning about the dangers of tobacco (executive summary, July 2011).